IEEE Access
Multidisciplinary | Rapid Review | Open Access Journal

Received August 24, 2021, accepted September 9, 2021, date of publication September 13, 2021,
date of current version September 22, 2021.

Digital Object Identifier 10.1109/ACCESS.2021.3112171

In-Fiber Mach–Zehnder Interferometer Based on Er Doped Up-Taper and Peanut-Shaped Fiber Structure in Fiber Ring Laser

WEIHAO LIN[1,2], SHENGJIE ZHOU[1], LI-YANG SHAO[1], (Senior Member, IEEE), MANG I. VAI[2], (Senior Member, IEEE), PERRY PING SHUM[1], (Senior Member, IEEE), FANG ZHAO[1], SHUAIQI LIU[1], (Graduate Student Member, IEEE), JIE HU[1], AND YUHUI LIU[1]

[1]Department of Electrical and Electronic Engineering, Southern University of Science and Technology, Shenzhen 518005, China
[2]Department of Electrical and Computer Engineering, Faculty of Science and Technology, University of Macau, Zhuhai, Macau

Corresponding author: Li-Yang Shao (shaoly@sustech.edu.cn)

This work was supported in part by the startup fund from the Southern University of Science and Technology, and in part by Shenzhen Government.

ABSTRACT It is demonstrated that in this paper a peanut shaped structure cascaded with up-taper fiber structure can realize the inter mode interference between the Erbium doped fiber (EDF) core mode and cladding modes in fiber ring laser (FRL). A simple and inexpensive Mach–Zehnder interferometer (MZI) based on this structure is proposed. Shown from experimental results, the optical intensity of the core mode can be coupled into the cladding modes in the first peanut-shaped structure. Then, the light in the cladding modes can be recoupled into the core mode in the up-taper structure. A high-quality interference spectrum with a signal to noise ratio about 50 dB was observed. Besides, the structure exhibits good mechanical stability when compared to MZIs based on taper or offset structure. The temperature sensitivity of the FRL sensor is 301 pm/°C and the RI sensitivity is 156 nm/RIU. This kind of MZI will have potential applications in remote sensing technique and the development of life and health.

INDEX TERMS Erbium doped fiber, fiber ring laser sensor, Mach–Zehnder interferometer.

I. INTRODUCTION

In the last few decades, the development of optical fiber-based interferometers has shown prospective results with high resolution and relatively low cost [1]–[3]. Various fiber-based interferometers play an important role in physical health monitoring techniques [4], marine monitoring [5] techniques, aquiculture [6], hazard forecasts [7], etc. Different kinds of structures have been proposed based on Michelson interferometer [8], Fabry-Perot interferometers (FPI) [9], fiber Bragg grating [10], etc. Besides, different structures of optic fiber temperature sensors based on the peanut-shaped fiber [11], up-taper fiber [12], and the air-cavity fiber structure [13] have been successfully proposed to improve the temperature sensitivity. The peanut shaped and up-taper shaped structure temperature sensor has the sensitivity of 73pm/°C and 43.2pm/°C, respectively. However, the mechanical properties of the sensing filter are significantly weakened while improving the sensing sensitivity. An extra noteworthy problem is that there are multiple interference peaks in the interference spectrum. These peaks will shift when the wavelength is affected by the external environment. If the wavelength shift is too large, it may cause the overlap of the two interference peaks, bringing errors and difficulties in detection. In order to overcome these shortcomings and obtain good sensing performance, fiber ring laser has been widely studied in recent years. Various types of Interferometer Fiber structures are embedded in the FRL to form a sensing system to measure biomolecules [14], magnetic field [15], electric field [16], stress [17], curvature [8], and environmental humidity [18]. In the sensing system, the interferometer plays a role of filtering, and its passband is affected by the exotic environment. Therefore, the laser, as an indicator of the sensor, can carry the information of external environment transformations. As for fiber ring laser system, narrow full width at half maxima and high SNR contribute to good sensing resolution, and a

The associate editor coordinating the review of this manuscript and approving it for publication was Muhammad Imran Tariq.

single peak value is easy to be detected. In view of the above advantages, the combination of fiber ring laser and modal interferometer is an effective way to improve the detection limit. In addition to the common interference fiber structure, embedding FBG [19] in the laser sensor is also used to improve the detection resolution. However, the additional modal interferometer will increase the loss and mechanical errors, which limits the sensitivity and practicability of the fiber ring laser sensor.

In this paper, we propose a new up-taper structure cascaded with a peanut structure based on Erbium doped fiber microspheres, which can realize the back-and-forth transformation of light intensity between the core mode and the cladding modes in the FRL. Consequently, a convenient and inexpensive MZI based upon peanut-shaped connecting with an up-taper structure working as both filter, sensor, and gain medium in EDF is achieved. To the best of our knowledge, the novelty peanut-shaped structures are used for the purpose of distributing part intensity of the cladding mode among the core modes. Besides, the up-taper structure is used as the beam splitter and combiner to re-catenate the optical intensity from the cladding modes to the core mode. The relative range between two structures is homologous with the coherence length of the MZIs. In the designed FRL sensor, the effective refractive index (RI) of cladding modes and core mode is different resulting in differences between two structures. Our research shows that the new peanut shaped structure combined with up-taper shaped can effectively inspire the cladding modes, thereby obtain a limpid interference pattern in the EDF composite structure. As a temperature sensor, the red shift of interference is observed, and the sensitivity is 301 pm/°c. Besides, as a RI sensing system, it's more durable than the interferometer on account of polished fiber and tapered structure, with a sensitivity about −156.2 nm/RIU which can be expected for highly sensitive temperature and RI monitoring.

II. SENSOR SETUP AND PRINCIPLE

As shown in Fig.1, shows the microstructure of the spherical peanut cascaded optical fiber Mach Zehnder interferometer. The input peanut fiber acts as a beam splitter and the output spherical structure acts as a coupler.

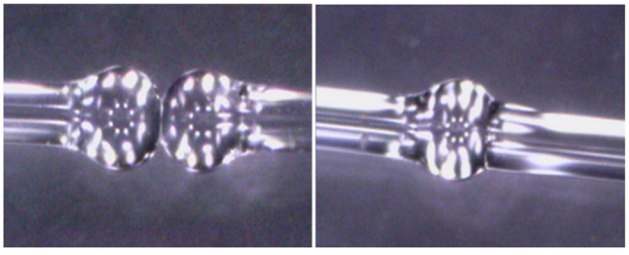

FIGURE 1. Microscope image of Er-doped fiber peanut-shaped and up-taper structure.

When the transmitted light travels to the input peanut-shaped fiber, the splitting effect occurs, leading part of the light in the core of the fiber to be coupled into the cladding of the Er-doped fiber for transmission, resulting in higher-order cladding modes. When light the transmitted to the output up-taper shaped fiber structure, the coupling effect occurs, in where the core mode and cladding modes form interference. There is an optical path difference between cladding and core, causing phase difference between cladding modes and core mode, the redistribution of light intensity energy, and the interference troughs of different peaks in the spectrum. To be more specific, first, the light field is transmitted in the fiber core in the form of the core mode. When the light field passes through the first microsphere, the cladding mode is excited due to the mismatch of core diameter. When the core mode and cladding mode arrive at the second microsphere, some higher-order cladding modes are re-coupled into the core at the junction of the second microsphere and the rare earth fiber. It then travels along the core and interferes with the core mold. Since the different phases depend on the mode state, there are phase differences between the different modes, as shown in Figure 2.

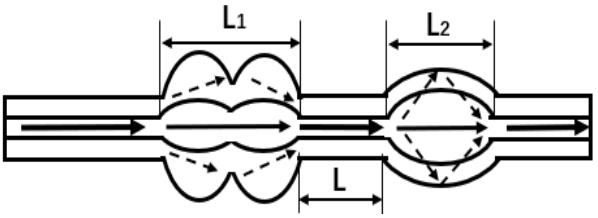

FIGURE 2. Schematic diagram of designed fiber structure.

If the core mode intensity of the fiber is I1 and the cladding mode intensity of the fiber is I2, the output intensity of the fiber sensor can be expressed as [20]:

$$I = I_1 + I_2 + 2\sqrt{I_1 I_2} COS\left[2\pi L\left(\frac{n_{eff}^{cl} - n_{cm,n}^{eff}}{\lambda}\right)\right] \quad (1)$$

where λ is the wavelength of the transmitted light, L is the length of the fiber between the spherical structure and the peanut-shaped structure, the effective RI of the core mode and J-order cladding mode is n_{eff}^{cl} and $n_{cm,n}^{eff}$,respectively. As the transmitted light passes through the sensor, the phase difference between the core mode and the J-order cladding modes can be expressed as:

$$\Delta\varphi = 2\pi L\left(n_{cl}^{eff} - n_{cm,n}^{eff}\right)/\lambda \quad (2)$$

$$\lambda_{dip} = 2L\left(n_{cl}^{eff} - n_{cm,n}^{eff}\right)/(2m+1) \quad (3)$$

The interference intensity is the minimum when m is an integer. The incident wavelength of transmitted light is one of the factors that determine the effective RI of cladding mode, moreover, related to the RI of the solution due to the direct contact between the cladding and the external environment. Correspondingly, the effective RI of the core mode is merely correlated with the transmitted light since there is no contact between the core and the solution.

The relationship between the sensitivity of characteristic wavelength and the temperature of the external environment can be expressed as follows:

$$\Delta\lambda \approx 2\lambda \left[\frac{1}{\Delta n_{eff}} \delta + k \right] \Delta T \tag{4}$$

where δ is the thermo optic coefficient of the fiber and k is the thermal expansion coefficient of the fiber. The variation of the effective RI of the core mode with the external ambient temperature satisfies equation 4, and the variation of the effective RI of the j-th cladding modes with the external ambient environment can be expressed as follows:

$$\Delta\lambda \approx \frac{-\lambda}{\Delta n_{eff}} \frac{\partial n_{eff}^{cl,n}}{\partial n_{RI}} \tag{5}$$

Fig.3 shows the diagram of the experimental device. The light is emitted from the laser and finally reaches the spectrometer with a resolution of 0.02nm (the spectrometer is Yokogawa AQ6370D). The two ends of the sensor are straightened and fixed on two fixed platforms with V-shaped grooves for heating. The main device in the experiment is a pump diode with a peak wavelength of 980nm (PL-974-500-FC/APC-P-M) and maximum pump energy of about 600 mW. A wavelength division multiplexer is used to connected the devices. The polarization controller is used to control the polarization state of the laser. Isolators are used for controlling the undirectional transmission of light. Fiber optic couplers are used to connect the Optical Spectrum Analyzer. The diameters of peanut microspheres are 200μm and 201μm, respectively. The center width of the joint point is 123μm. The spherical structure is made of fused optical fibers with a diameter of 200 μm and 20mm of coherent length as mentioned in Fig.2.

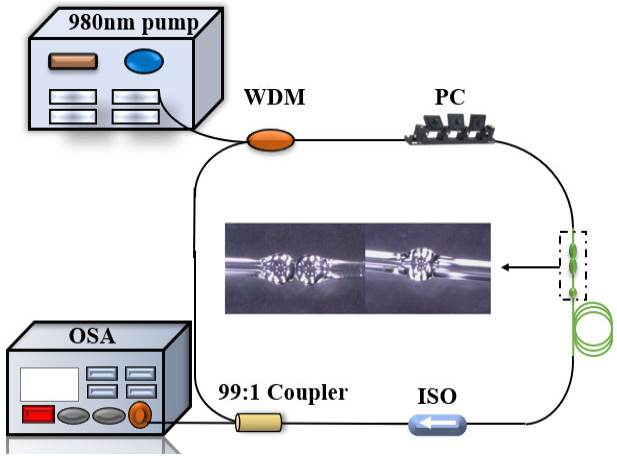

FIGURE 3. Diagram of optical fiber laser sensor device.

An EDF (Thorlabs θ M5-980-125) with a total length of 1.6m was truncated into three segments, and the erbium-doped peanut structure and up-tapered fiber structure were prepared, respectively. For the fabrication process of the peanut shaped structure, firstly, the coating of erbium-doped fiber is stripped and wiped with alcohol. Then use the optical fiber cutting machine to cut the optical fiber end flat. Then put the two optical fiber ends into the optical fiber connector, and the fiber splicer is set to the manual motor drive state. Adjust the two end faces of the optical fiber to the appropriate position, two end faces can be seen on the plane of the optical fiber welding machine. Set the discharge power and discharge time (800ms), discharge and repeat the operation for 10 times. The two ends are heated and softened. Due to the surface tension of the material itself, the fiber end face gradually tends to arc shape during cooling. Moreover, other ellipsoidal types of fiber are also fabricated by the same method. The two shapes of fiber are spliced by electric discharge. The same treatment is also applied to the microspheres.

The selection of peanut structure parameters is based on the use of different welding parameters to weld the optical fiber, increase the discharge and discharge time of the first welding, make different diameter of the ball, use the manual welding mode described in the previous section, make different diameter of peanut sensor. The diameter of the optical fiber sensing head is 185μm, 190μm, 200μm and 215μm, respectively. The sensor head is installed in a computer-controlled thermostat. The interference signal with the temperature information is output to the optical Spectrum analysis. The temperature information is measured through the change of wavelength. As the temperature increases, the interference peak shifts (red shift) in the direction of larger wavelength. When the sensor diameter increases from 185μm to 200μm, the wavelength drift of the interference peak increases with the increase of the diameter and the same temperature range. However, when the diameter is 215μm, the temperature shift decreases. One reason is that the peanut diameter larger, in the melt contact will inspire more cladding mode, and increase the percentage of light into the cladding, the second reason is when the larger diameter welding type peanut structure, put the battery needs to be increased, the refractive index of fiber core and cladding fiber melting changes, narrowing of the refractive index of fiber core and cladding, As the diameter increases, the light excites more higher-order modes, and the effect on the sensitivity becomes more complex.

The FRL sensing system is shown in Fig.3. A spectrum analyzer is selected to monitor the interference spectrum in the manufacturing process of MZI in FRL sensing system. The sensing part of optical fiber is ellipsoidal micro lens, which are composed of two ellipsoidal micro lenses and a microsphere lens. As the sensing unit, erbium-doped fiber offers three advantages. First of all, no additional filter is needed to simplify the system and improve the stability. Secondly, the thermal expansion coefficient of erbium-doped fiber is larger than that of ordinary fiber, and the detection sensitivity is improved by 1-2 orders of magnitude. Finally, Er-doped fiber can be used as both sensing unit and gain medium to effectively reduce the product price.

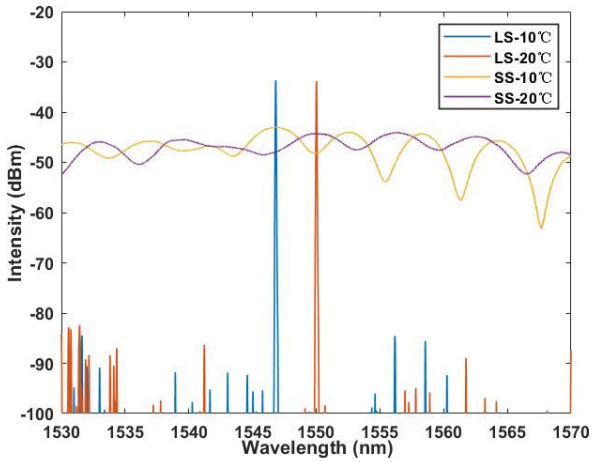

FIGURE 4. Output spectrum of the sensor in SS (super-continuum light source) and LS (laser source).

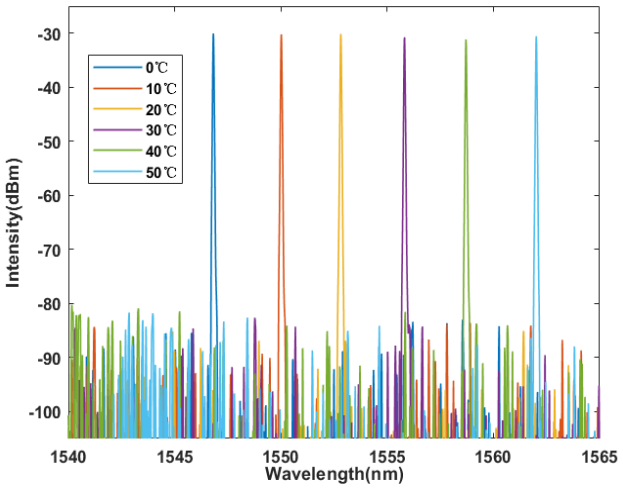

FIGURE 5. Output spectrum of the fiber laser temperature sensor system when T changes from 0°C to 50°C with the steps of 10°C.

III. EXPERIMENTAL RESULTS AND DISCUSSION

Fig.4 shows the corresponding relationship between broadband light source and laser. It can be found that there is a good correspondence between the broad light spectrum and the laser output spectrum at room temperature.

Shown in Fig.5 and Fig.6, is the output spectrum of the sensor at different temperatures. With the increasing temperature of the electric furnace, the phenomenon of red shift appears that the interference troughs are obviously drifting towards the long wave direction. As shown in Fig.6, when the temperature rises from 0°C to 50°C, the characteristic wavelength of the laser has a red shift about 14nm, it can be calculated that the temperature sensitivity reaches 301 pm/°C, and the corresponding temperature linear fitting coefficient is 0.99948.

The refractive index solution used in the experiment is made of distilled water and glycerin solution, whose refractive index range from 1.3428 to 1.3927. The RI is calibrated and measured by refractive index calibrator. Fig.7 shows the

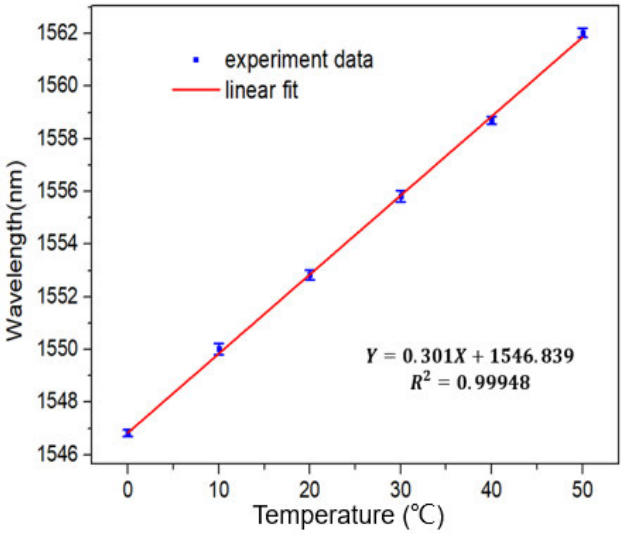

FIGURE 6. Linear fitting and error bars of the relationship between temperature and wavelength shift. (From 0°C-50°C).

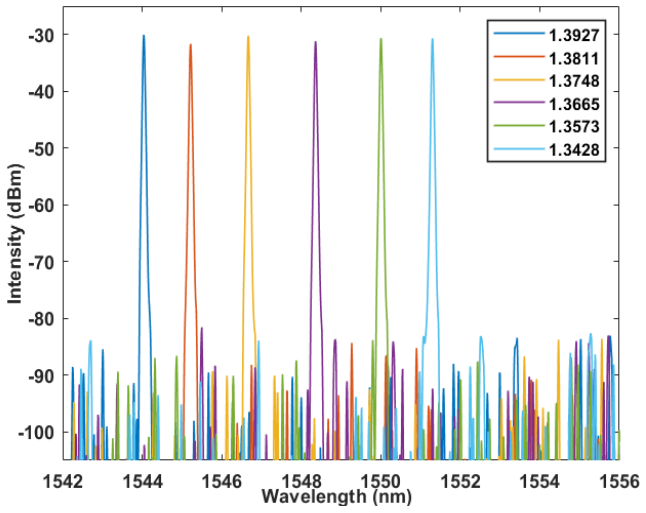

FIGURE 7. Laser emission spectra due to RI changes with surrounding mediums.

spectrum of laser output peak varying with external RI. As the refractive index increases, the wavelength moves towards the shorter wavelength. As shown in Fig.8. When the external RI changes from 1.3428 to 1.3927, the laser peak shifts to the short-wave direction about 17nm. It can be calculated that the RI sensitivity reaches −156.128nm/RIU, and the corresponding linear fitting coefficient was 0.97245. The offset of the output wavelength has a good linear fit with RI.

The power fluctuation and wavelength change are plotted in Figure 9 for quantitative analysis of FRL sensing system stability. In 3.5 hours, the intensity stability of different solutions is stable with only 1.5 dBm changes, and the wavelength change is less than 0.3 nm which the possibility of the sensor as a stable sensor filter is verified. The test is carried out at the refractive index value equals to 1.3811.

In addition, table 1 and table 2 respectively compare the sensitivity of the designed sensor with other sensing systems.

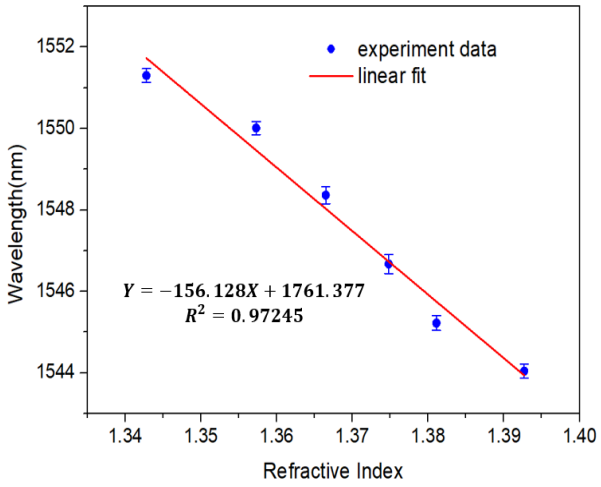

FIGURE 8. Linear fitting and error bars of the relationship between RI and wavelength shift.

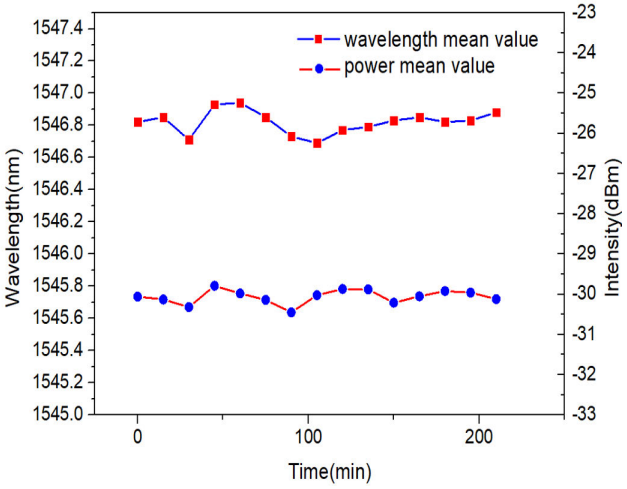

FIGURE 9. Test for time stability of wavelength shift and power fluctuation.

TABLE 1. Sensitivity comparison with other temperature sensing structures.

Structures	Sensitivity(nm/℃)	Refs.
SMF-MZI	0.07	[21]
EDF-MZI	0.158	[22]
Up-Taper fiber structure	0.092	[23]
Hybrid Cavity and a Random Mirror	0.006	[24]
Current work	0.301	

The results show that the designed FRL sensor has great temperature and refractive index sensing characteristics.

Compared with the traditional fiber ring laser using FBG for temperature sensing [28], the designed sensor does not require additional filter design, and the sensitivity is better than FBG. Besides, the fiber laser temperature sensor based on liquid filling or Sagnac loop can effectively improve the sensitivity [29]–[31]. But it increases the cost of system design and reduces the stability. The sensor can also be used as a gain medium to pump the laser.

TABLE 2. Sensitivity comparison with other temperature sensing structures.

Structures	Sensitivity(nm/RIU)	Refs.
Micro-fiber	50.45	[21]
tapered-MZI	158	[22]
Up-Taper fiber structure	19	[23]
LPFG	58.5	[24]
Current work	156	

IV. CONCLUSION

An Erbium doped FRL sensing system is demonstrated theoretically and experimentally. The modal MZI of peanut structure cascaded with up-taper joints structure is inserted into the FRL as sensing element, gain medium and filter. Consequently, the sensing system also possesses the ability to react to ambient environments with ultra-high sensitivities. The characteristics of temperature and RI are also tested and the sensitivities are 301pm/°C and 156 nm/RIU, respectively. In addition, the MZI has the advantages a narrower 3 dB bandwidth (∼0.1 nm) and a higher OSNR (∼50 dB), easy fabrication, and a low-cost sensing process, which makes it attractive for remote sensing technology and extreme environmental monitoring.

ACKNOWLEDGMENT

(Weihao Lin and Shengjie Zhou contributed equally to this work.)

REFERENCES

[1] H. W. Lee, M. A. Schmidt, P. Uebel, H. Tyagi, N. Y. Joly, M. Scharrer, and P. S. J. Russell, "Optofluidic refractive-index sensor in step-index fiber with parallel hollow micro-channel," *Opt. Exp.*, vol. 19, no. 9, pp. 8200–8207, Apr. 2011.

[2] M. Quan, J. Tian, and Y. Yao, "Ultra-high sensitivity Fabry–Pérot interferometer gas refractive index fiber sensor based on photonic crystal fiber and Vernier effect," *Opt. Lett.*, vol. 40, no. 21, pp. 4891–4894, Nov. 2015.

[3] R. Lv, J. Li, H. Hu, and C. Yao, "Miniature refractive index fiber sensor based on silica micro-tube and Au micro-sphere," *Opt. Mater.*, vol. 72, pp. 661–665, Oct. 2017.

[4] J. Li, J. Chen, and F. Xu, "Sensitive and wearable optical microfiber sensor for human health monitoring," *Adv. Mater. Technol.*, vol. 3, no. 12, Dec. 2018, Art. no. 1800296.

[5] R. A. Beach, R. W. Sternberg, and R. Johnson, "A fiber optic sensor for monitoring suspended sediment," *Mar. Geol.*, vol. 103, nos. 1–3, pp. 513–520, Jan. 1992.

[6] C. Shi, H. Qi, R. Ma, Z. Sun, L. Xiao, G. Wei, Z. Huang, S. Liu, J. Li, M. Dong, J. Fan, and Z. Guo, "N,S-self-doped carbon quantum dots from fungus fibers for sensing tetracyclines and for bioimaging cancer cells," *Mater. Sci. Eng. C, Mater. Biol. Appl.*, vol. 105, Dec. 2019, Art. no. 110132.

[7] Z. Li, Y. Zhou, B. Jiang, X. Gan, L. Yan, and J. Zhao, "Phase fluctuation cancellation for coherent-detection BOTDA fiber sensors based on optical subcarrier multiplexing," *Opt. Lett.*, vol. 46, no. 4, pp. 757–760, Feb. 2021.

[8] K. Qi, Y. Zhang, J. Sun, Y. Guo, F. Zhu, H. Su, and G. Yi, "High-performance bending sensor based on fiber microspheres array Michelson interferometer," *IEEE Sensors J.*, vol. 21, no. 5, pp. 6145–6151, Mar. 2021.

[9] T. T. Gang, R. X. Tong, and C. Bian, "A novel strain sensor using a fiber taper cascaded with an air bubble based on Fabry–Pérot interferometer," *IEEE Sensors J.*, vol. 21, no. 4, pp. 4618–4622, Feb. 2021.

[10] L. Xiong, Y. Guo, G. Jiang, X. Zhou, L. Jiang, and H. Liu, "Six-dimensional force/torque sensor based on fiber Bragg gratings with low coupling," *IEEE Trans. Ind. Electron.*, vol. 68, no. 5, pp. 4079–4089, May 2021.
[11] F. Yu, P. Xue, X. Zhao, and J. Zheng, "Investigation of an in-line fiber Mach–Zehnder interferometer based on peanut-shape structure for refractive index sensing," *Opt. Commun.*, vol. 435, pp. 173–177, Mar. 2019.
[12] X. Han, C. Liu, S. Jiang, S. Leng, and J. Yang, "Up-down taper based in-fiber Mach–Zehnder interferometer for liquid refractive index sensing," *Sensors*, vol. 19, no. 24, p. 5440, Dec. 2019.
[13] X. L. Cui and D. N. Wang, "Fiber in-line interferometer based on air-cavity with suspended fiber-core for sensing," *Meas. Sci. Technol.*, vol. 31, no. 10, Oct. 2020, Art. no. 105103.
[14] M. Mansor, M. H. A. Bakar, M. F. Omar, Y. M. Kamil, N. H. Z. Abidin, F. H. Mustafa, and M. A. Mahdi, "Taper biosensor in fiber ring laser cavity for protein detection," *Opt. Laser Technol.*, vol. 125, May 2020, Art. no. 106033.
[15] Y. Chen, Q. Han, W. Yan, M. Xu, and T. Liu, "Magnetic field sensing based on a ferrofluid-coated multimode interferometer in a fiber-loop ring-down cavity," *IEEE Sensors J.*, vol. 18, no. 8, pp. 3206–3210, Apr. 2018.
[16] R. Qiu, H. Lin, J. Huang, C. Liang, and Z. Yi, "Tunable multipolar Fano resonances and electric field enhancements in Au ring-disk plasmonic nanostructures," *Materials*, vol. 11, no. 9, p. 1576, Sep. 2018.
[17] S. Li, X. Li, Y. Qin, and Y. Zhao, "Local strain gauge based on the nanowires ring resonator embedded in a flexible substrate," *Micro Nano Lett.*, vol. 15, no. 14, pp. 1028–1032, Dec. 2020.
[18] M. Madry, L. Alwis, L. Binetti, L. Pajewski, and E. Beres-Pawlik, "Simultaneous measurement of temperature and relative humidity using a dual-wavelength erbium-doped fiber ring laser sensor," *IEEE Sensors J.*, vol. 19, no. 20, pp. 9215–9220, Oct. 2019.
[19] J. Shi, F. Yang, W. Xu, D. Xu, H. Bai, C. Guo, Y. Wu, S. Zhang, T. Liu, and J. Yao, "High-resolution temperature sensor based on intracavity sensing of fiber ring laser," *J. Lightw. Technol.*, vol. 38, no. 7, pp. 2010–2014, Apr. 1, 2020.
[20] C. Sun, M. Wang, J. Liu, S. Ye, L. Liang, and S. Jian, "Fiber ring cavity laser based on modal interference for curvature sensing," *IEEE Photon. Technol. Lett.*, vol. 28, no. 8, pp. 923–926, Apr. 15, 2016.
[21] Y. Geng, X. Li, X. Tan, Y. Deng, and Y. Yu, "High-sensitivity Mach–Zehnder interferometric temperature fiber sensor based on a waist-enlarged fusion bitaper," *IEEE Sensors J.*, vol. 11, no. 11, pp. 2891–2894, Nov. 2011.
[22] W. Lin, L.-Y. Shao, M. I. Vai, P. P. Shum, S. Liu, Y. Liu, F. Zhao, D. Xiao, Y. Liu, Y. Tan, and W. Wang, "In-fiber Mach–Zehnder interferometer sensor based on Er doped fiber peanut structure in fiber ring laser," *J. Lightw. Technol.*, vol. 39, no. 10, pp. 3350–3357, May 15, 2021.
[23] Y. Zhao, L. Cai, and X.-G. Li, "In-fiber Mach–Zehnder interferometer based on up-taper fiber structure with Er^{3+} doped fiber ring laser," *J. Lightw. Technol.*, vol. 34, no. 15, pp. 3475–3481, Aug. 1, 2016.
[24] A. M. R. Pinto, M. Lopez-Amo, J. Kobelke, and K. Schuster, "Temperature fiber laser sensor based on a hybrid cavity and a random mirror," *J. Lightw. Technol.*, vol. 30, no. 8, pp. 1168–1172, Apr. 15, 2012.
[25] H. Su and F. Zhou, "Optimization of micro-optical fiber-based Mach–Zehnder interferometer RI sensor," *J. Lightw. Technol.*, vol. 36, no. 18, pp. 4039–4045, Sep. 15, 2018.
[26] Q. Wang, W. Wei, M. Guo, and Y. Zhao, "Optimization of cascaded fiber tapered Mach–Zehnder interferometer and refractive index sensing technology," *Sens. Actuators B, Chem.*, vol. 222, pp. 159–165, Jan. 2016.
[27] Y.-E. Fan, T. Zhu, L.-L. Shi, and Y.-J. Rao, "Highly sensitive refractive index sensor based on two cascaded special long-period fiber gratings with rotary refractive index modulation," *Appl. Opt.*, vol. 50, no. 23, pp. 4604–4610, Aug. 2011.
[28] S. Diaz, N. S. Fabian, A. B. Socorro-Leranoz, and I. R. Matias, "Temperature sensor using a multiwavelength erbium-doped fiber ring laser," *J. Sensors*, vol. 2017, pp. 1–6, Jan. 2017.
[29] W. Lin, Y. Liu, L. Shao, and M. I. Vai, "A fiber ring laser sensor with a side polished evanescent enhanced fiber for highly sensitive temperature measurement," *Micromachines*, vol. 12, no. 5, p. 586, May 2021.
[30] W. Lin, L. Shao, L. Yibin, S. Bandyopadhyay, L. Yuhui, X. Weijie, L. Shuaiqi, H. Jie, and M. I. Vai, "Temperature sensor based on fiber ring laser with cascaded fiber optic Sagnac interferometers," *IEEE Photon. J.*, vol. 13, no. 2, pp. 1–12, Apr. 2021.
[31] X. Yang, Y. Lu, B. Liu, and J. Yao, "Fiber ring laser temperature sensor based on liquid-filled photonic crystal fiber," *IEEE Sensors. J.*, vol. 17, no. 21, pp. 6948–6952, Nov. 2017.

WEIHAO LIN received the B.Eng. degree in optoelectronic information science and engineering from the Southern University of Science and Technology, China, in 2019. He is currently pursuing the Ph.D. degree under a collaboration program between the Southern University of Science and Technology and the University of Macau. His research interests include optical fiber sensor, fiber laser sensors, and fiber lasers.

SHENGJIE ZHOU is currently pursuing the B.Eng. degree in electronic and electrical engineering the Southern University of Science and Technology, China.

LI-YANG SHAO (Senior Member, IEEE) received the Ph.D. degree in optical engineering from Zhejiang University, China, in 2008. From 2006 to 2009, he was with The Hong Kong Polytechnic University, as a Research Assistant/Associate, working on fiber grating devices and sensors. Then, he was a Postdoctoral Fellow with the Department of Electronics, Carleton University, Canada. In 2011, he returned to The Hong Kong Polytechnic University for another Postdoctoral Research Project. In 2012, he was granted the Endeavor Research Fellowship from the Australian Government and working with the Interdisciplinary Photonics Laboratory, The University of Sydney. In 2013, he joined Southwest Jiaotong University, as a Full Professor. In 2017, he joined the Department of Electrical and Electronic Engineering, Southern University of Science and Technology, where he became the Associate Dean of the School of Innovation and Entrepreneurship, in 2018. He has authored or coauthored more than 150 articles in the refereed international journals/conferences with a total citation of more than 2800 times (SCI citation of over 1800 times by the other researchers). His research interests include fiber grating and sensors, distributed fiber optic sensing, microwave photonics for sensing, and smart sensing systems for railway industry. He acts as the Principal Investigator for several high-level projects, such as NSFC Projects and International S&T Cooperation Program of China. He was a TPC or Organizing Committee Member of multiple conferences, including ICAIT (2009–2013), PGC 2010, OFS 2011, PIERS 2014, ICOCN (2015–2016), PGC 2017, APOS 2018, CLEO-PR 2018, ACP 2019, APOS 2019, and CLEO-PR 2020. He serves as a Reviewer for more than 20 SCI journals, including *Optics Letters*, *Optics Express*, the *Journal of Lightwave Technology*, and the IEEE PHOTONICS TECHNOLOGY LETTERS.

MANG I. VAI (Senior Member, IEEE) received the Ph.D. degree in electrical and electronics engineering from the University of Macau, China, in 2002.

He is currently a Coordinator with the State Key Laboratory of Analog and Mixed-Signal VLSI and an Associate Professor of electrical and computer engineering with the Faculty of Science and Technology, University of Macau. Since 1984, he has been performing research in the areas of digital signal processing and embedded systems.

PERRY PING SHUM (Senior Member, IEEE) received the B.Eng. and Ph.D. degrees in electronic and electrical engineering from the University of Birmingham, Birmingham, U.K., in 1991 and 1995, respectively. In 1999, he joined the School of Electrical and Electronic Engineering, Nanyang Technological University, Nanyang, China. He has authored or coauthored more than 400 international journal and conference papers. His research interests include concerned with optical communications, fiber sensors, and fiber lasers. He is the technical program chair, a committee member, and an international advisor of many international conferences.

FANG ZHAO is currently pursuing the Ph.D. degree in electronic and electrical engineering with the Southern University of Science and Technology, China.

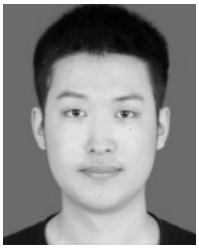

SHUAIQI LIU (Graduate Student Member, IEEE) received the bachelor's degree in optoelectronic information science and engineering from Nanjing University, in 2018. He is currently pursuing the Ph.D. degree under a collaboration program between the Southern University of Science and Technology and Macau University of Science and Technology.

JIE HU received the bachelor's and master's degrees in optical information science and technology from China Jiliang University, in 2016 and 2019, respectively. He is currently pursuing the Ph.D. degree with the Southern University of Science and Technology.

YUHUI LIU received the B.Eng. degree in optoelectronic information science and engineering from the Southern University of Science and Technology, China, in 2019. She is currently pursuing the Ph.D. degree under a collaboration program between the Southern University of Science and Technology and The Hong Kong Polytechnic University.